

GRIP1 and 2 regulate activity-dependent AMPA receptor recycling via exocyst complex interactions

Lifang Mao¹, Kogo Takamiya², Gareth Thomas, Da-Ting Lin³, and Richard L. Huganir⁴

Department of Neuroscience and The Howard Hughes Medical Institute, The Johns Hopkins University School of Medicine, Baltimore, MD 21205

Contributed by Richard L. Huganir, September 23, 2010 (sent for review August 26, 2010)

PSD-95/SAP90/DLG/ZO-1 (PDZ) domain-mediated protein-protein interactions play important roles in regulating AMPA receptor trafficking and neuronal plasticity. GRIP1 and GRIP2 are homologous multi-PDZ domain-containing proteins that bind to the C-termini of AMPA-R GluA2 and GluA3 subunits. Previous attempts to determine the cellular roles of GRIP1 and GRIP2 in neurons have been complicated by nonspecific reagents, and by the embryonic lethality of conventional GRIP1 KO mice. To circumvent these issues we developed a conditional targeted deletion strategy to knock out GRIP1 in postnatal neurons derived from GRIP2 KO mice. Loss of GRIP1 and 2 did not affect normal AMPA-R steady-state trafficking and endocytosis, but strikingly impaired activity-dependent AMPA-R recycling. This previously uncharacterized role for GRIP1 appears to be mediated by novel interactions with the cellular trafficking machinery via the exocyst protein complex. Indeed, disruption of GRIP1-exocyst binding caused a strikingly similar deficit in AMPA-R recycling. Together these findings reveal a previously unidentified role for AMPA-R-GRIP1-exocyst protein complexes in activity-dependent AMPA-R trafficking.

endocytosis | KO | long-term depression | PSD-95/SAP90/DLG/ZO-1 | NMDA

AMPA receptors conduct the majority of fast excitatory synaptic transmission in the mammalian central nervous system. Dynamic regulation of AMPA-R trafficking in and out of synapses modulates the efficacy of synaptic transmission and is crucial for synaptic plasticity (1–3). One major molecular mechanism that governs AMPA-R trafficking is the regulated interaction of intracellular C-termini of AMPA-R subunits with PSD-95/SAP90, DLG/ZO-1 (PDZ) domain-containing proteins (4–7). The type II PDZ motifs of GluA2 and GluA3 C-termini interact with several PDZ domain-containing proteins, including PICK1 (6, 7) and the homologous GRIP1 and GRIP2 proteins (GRIP2 is also called ABP for AMPA-R binding protein) (4, 5, 8, 9). GRIP proteins and PICK1 interact with GluA2 at the same site, but are differentially regulated by PKC-dependent phosphorylation of GluA2 Ser880 (10–12). In addition to GluA2/3, GRIP1 and 2 binds various signaling and cytoskeletal proteins, including EphB receptor tyrosine kinase, ephrinB ligands, α -liprin scaffolding protein, proteoglycan NG2, Fras1 and 2, GRIP1-associated protein 1 (GRASP-1), kinesin-1/KIF5 microtubule motor protein and matrix metalloproteinase 5 (13–19). Thus, GRIP proteins may serve to organize macromolecular complexes, linking AMPA-Rs and other membrane proteins to the cytoskeleton and membrane trafficking and signal transduction pathways.

GRIP-GluA2/3 interactions are implicated in regulating AMPA-R synaptic targeting. Overexpression of the GluA2 C terminus in neurons decreases the synaptic targeting of AMPA-Rs (4). Point mutants of GluA2 that are unable to bind GRIP proteins exhibit reduced synaptic accumulation (20). GRIP1's sixth PDZ domain interacts with the α -liprin family of proteins, and disrupting GRIP- α -liprin interactions inhibits AMPA-R surface expression and synaptic targeting (14). GRIP proteins also bind kinesin heavy chain, an interaction that is reported to control transport of AMPA-Rs into dendrites (17). These data suggest that GRIP proteins act in the transport and maintenance of AMPA-Rs at synapses. However, some results point to different

roles of GRIP proteins in AMPA-R trafficking. Perfusion of hippocampal CA1 pyramidal neurons with a peptide that disrupts GluA2-GRIP interactions potentiates basal EPSCs, suggesting that GRIP proteins retain AMPA-Rs intracellularly (21). GRIP1 binding to the endosomal protein NEEP21 is also reported to regulate AMPA-R sorting and recycling (22, 23). GRIP1 has also been reported to bind PICK1 to initiate the endocytosis of GluA2-containing AMPA-Rs (24). Genetic deletion of GRIP1 and GRIP2 blocks long-term depression (LTD) in cerebellar Purkinje cells, a process dependent on AMPA-R endocytosis. These data indicate that GRIP proteins regulate AMPA-R endocytosis and recycling.

In this study, we used GRIP1 conditional KO and GRIP2 conventional KO mice to study the neuronal function of GRIP1 and GRIP2. Cortical and hippocampal neurons were cultured from these mutant mice and the GRIP1 gene was deleted by high-efficiency lentiviral infection of Cre recombinase. AMPA-R steady-state trafficking, synaptic targeting, and basal endocytosis were all normal in GRIP1 and 2 double KO (DKO) neurons. However, both biochemical and imaging analyses revealed that GRIP1 deletion greatly slowed AMPA-R recycling following NMDA-R-induced endocytosis of GluA2, without affecting the kinetics of endocytosis. We identified an interaction between GRIP1 and exocyst proteins *in vitro* and *in vivo*, which may mediate this effect. Indeed, disruption of the interaction between GRIP1 and Sec8, a core exocyst protein, similarly attenuated NMDA-R-mediated GluA2 recycling. Together, these data suggest that a previously uncharacterized GRIP1-exocyst complex is a key controller of NMDA-R-dependent AMPA-R trafficking.

Results

Virally Mediated Deletion of GRIP1 in Cultured Neurons. To directly examine the roles of GRIP1 and GRIP2 in AMPA-R trafficking, neuronal cultures were prepared from GRIP1 conditional (flo^x/flo^x) and GRIP2 conventional (^{-/-}) KO mice. GRIP1 (flo^x/flo^x) and GRIP2 (^{-/-}) mutant mice were viable (16, 25), and were intercrossed to produce GRIP1 (flo^x/flo^x) and GRIP2 (^{-/-}) double mutant mice. Lentiviruses for the expression of Cre recombinase (Cre-GFP, Cre only, and GFP-IRES-Cre) and GFP control were introduced into cortical cultures from GRIP1 (flo^x/flo^x) and GRIP2 (^{-/-}) double mutant mice. As previously described, complete loss of GRIP1

Author contributions: L.M., K.T., D.-T.L., and R.L.H. designed research; L.M., K.T., and D.-T.L. performed research; L.M. and K.T. contributed new reagents/analytic tools; L.M. and D.-T.L. analyzed data; and L.M., K.T., G.T., and R.L.H. wrote the paper.

Conflict of interest statement: Under a licensing agreement between Millipore, Inc., and The Johns Hopkins University, Dr. Huganir is entitled to a share of royalty received by the University on sales of products described in this article. Dr. Huganir is a paid consultant to Millipore, Inc. The terms of this arrangement are being managed by the Johns Hopkins University in accordance with its conflict of interest policies.

¹Present address: Department of Neurology, University of California, San Francisco, CA 94143-2922.

²Present address: Department of Integrative Physiology, University of Miyazaki Faculty of Medicine, Miyazaki 889-1692, Japan.

³Present address: Jackson Laboratory, Bar Harbor, ME 04609.

⁴To whom correspondence should be addressed. E-mail: rhuganir@jhmi.edu.

This article contains supporting information online at www.pnas.org/lookup/suppl/doi:10.1073/pnas.1013494107/-DCSupplemental.

protein was observed only 7–10 d after Cre lentivirus infection (25). We therefore routinely applied lentiviruses to neurons at DIV 1–4 and performed analyses ≥ 7 d (normally 10 d) later. Complete loss of GRIP1 protein was confirmed by Western blotting of each murine culture preparation (Fig. S1A).

Steady-State Surface Expression of AMPA-Rs in GRIP1 and GRIP2 KO Neurons.

First, we examined AMPA-R surface expression in GRIP1 and GRIP2 KO neurons. Cortical cultures were prepared from WT and GRIP1(flox/flox) and GRIP2($^{-/-}$) mice and both were infected with Cre lentiviruses (wt vs. GRIP1 and 2 DKO). At the same time, GRIP1(flox/flox) and GRIP2($^{-/-}$) cortical cultures were infected with GFP or Cre-GFP lentiviruses to check the difference between GRIP2 KO and GRIP1 and 2 DKO. After complete disappearance of GRIP1 protein, we examined receptor levels on the cell surface at steady state using biotinylation assays (26, 27). Surface expression of AMPA-R GluA2 and GluA3 subunits in cortical neurons lacking both GRIP1 and GRIP2 were comparable to the GRIP2 KO and WT neurons (GRIP1 and 2 DKO: GluA2: 90.0% \pm 3.0%, GluA3: 98.2% \pm 1.9%; GRIP2 KO: GluA2: 92.1% \pm 3.9%, GluA3: 90.0% \pm 4.9%, relative to that of the WT) ($n = 6$) (Fig. S1B and C).

Previous studies suggest that GRIP1 and GRIP2 act as scaffolding proteins to anchor AMPA-Rs at the cell surface and synapses (4, 20). Although there was no change in the steady-state surface expression of AMPA-R GluA2 and GluA3 subunits in GRIP1 and 2 KO neurons, it was still possible that AMPA-R synaptic targeting could be affected by receptor redistribution between synapses and extrasynaptic sites. To test this possibility, we examined GluA1 and GluA2 localization in low-density hippocampal cultures prepared from WT and GRIP1 and 2 DKO mice. In GRIP1 and 2 DKO neurons, surface GluA1 still colocalized extensively with a postsynaptic marker PSD-95 (Fig. S1D, a–f). GluA2 also coclustered with surface GluA1 puncta in GRIP1 and 2 DKO neurons (Figs. 1D, g–i), demonstrating that AMPA-Rs are still targeted to synapses in the absence of GRIP1 and GRIP2.

Basal and NMDA-Induced AMPA-R Endocytosis and Recycling in GRIP1 and GRIP2 Knockout Neurons.

Biotinylation assays were used to examine the basal endocytosis of AMPA-R GluA2 subunit in WT, GRIP2 KO, and GRIP1 and 2 DKO neurons (27). Neurons were treated with Sulfo-NHS-SS-Biotin, incubated for the indicated times to allow endocytosis, and the remaining surface biotin was cleaved from the labeled proteins using glutathione. The endocytosed biotinylated proteins were then isolated using NeutraAvidin agarose beads and analyzed. Quantitative Western blotting revealed that there was no difference in endocytosis between the KOs and WT neurons (GRIP1 and 2 DKO: 92.0% \pm 4.6%, GRIP2 KO: 91.6% \pm 6.9%, relative to that of the WT) ($n = 3$) (Fig. 1A and D). Together, these data suggest that GRIP1 and GRIP2 do not regulate steady-state AMPA-R trafficking and synaptic targeting in neurons.

However, several previous studies suggest that GRIP1 and GRIP2 control activity-regulated AMPA-R trafficking and thus affect synaptic plasticity (21, 25, 28, 29). Application of NMDA to neurons results in endocytosis and subsequent recycling of AMPA-Rs to the surface. This process involves signaling mechanisms shared with NMDA-R-dependent LTD, and is thus regarded as a model of LTD (27, 30–32). To examine NMDA-induced AMPA-R endocytosis upon GRIP1 and 2 deletion, we first checked the time course of NMDA-induced AMPA-R endocytosis/recycling. AMPA-Rs were maximally internalized 10 min after NMDA treatment and returned to the cell surface after 35 min (Fig. 1B). Using the 10-min time point, biotinylation assays of NMDA-induced endocytosis were performed on WT, GRIP2 KO, and GRIP1 and 2 DKO neurons to check GluA2 endocytosis. No significant difference was found between KO and WT

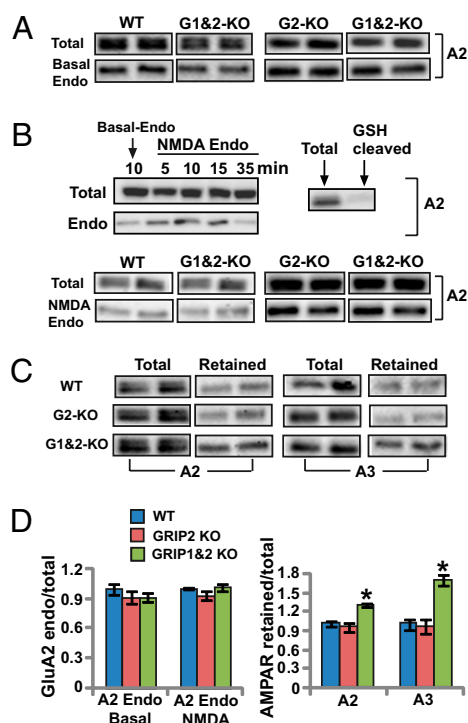


Fig. 1. AMPA-R endocytosis and recycling in GRIP KO neurons. (A) GluA2 basal endocytosis in GRIP1 and 2 KO neurons. Biotin-labeled surface AMPA-Rs were allowed to internalize for 30 min at 37 °C. Representative Western blots of duplicate samples of total (Top) and internalized (Bottom) GluA2 subunit are shown. A2, GluA2; A3, GluA3; WT: WT, G2-KO: GRIP2 KO, G1&2-KO: GRIP1 and 2 KO, Endo: endocytosis. (B) NMDA-induced GluA2 endocytosis in GRIP1 and 2 KO neurons. (Top Left) WT mouse cortical neurons were treated with NMDA for 3 min and subsequently incubated 5, 10, 15, and 35 min (lane 2–5) to examine the time course of AMPA-R internalization. Lane 1 is a control with 10-min basal endocytosis without NMDA treatment. Western blotting shows the total and internalized GluA2. To confirm the cleavage efficiency of Sulfo-NHS-SS-Biotin, neurons were surface biotinylated and immediately incubated with glutathione cleavage buffer (Top Right). Western blotting shows the biotin-labeled GluA2. (Bottom), biotin-labeled AMPA-Rs in WT, GRIP2 KO, and GRIP1 and 2 KO neurons were treated with NMDA for 3 min and then allowed to internalize for 10 min. Representative Western blots of duplicate samples of total and internalized GluA2 are shown. (C) NMDA-induced GluA2 recycling in GRIP1 and 2 KO neurons. After surface biotinylation, WT, GRIP2 KO and GRIP1 and 2 KO neurons were treated with NMDA for 3 min and then incubated for 30 min to allow endocytosis/recycling of AMPA-Rs. Representative Western blots of duplicate samples for total and intracellularly retained GluA2 (Left) and GluA3 (Right) are shown. (D) Quantitation of AMPA-R endocytosis and recycling. Endocytosis and recycling levels were calculated as the ratio of internalized/total AMPA-Rs and normalized to that of the WT. Histograms represent mean \pm SEM derived from A for GluA2 basal endocytosis (Left, $n = 3$), from B for NMDA-induced GluA2 endocytosis (Left, $n = 3$), and from C for NMDA-induced GluA2 and GluA3 recycling (Right graphs, * $P < 0.05$ compared with the GRIP2 KO and the WT, t test, $n = 5$).

neurons (GRIP1 and 2 DKO: 101.6% \pm 3.6%; GRIP2 KO: 93.4% \pm 4.5%, relative to that of WT) ($n = 3$) (Fig. 1B and D).

Next, we examined AMPA-R recycling after NMDA treatment. Internalized AMPA-Rs recycle back to the cell surface 15–35 min after NMDA treatment (Fig. 1B). Because NMDA-induced AMPA-R endocytosis is unaltered in GRIP1 and 2 DKO neurons, AMPA-R recycling can be determined by examining the retention of internalized AMPA-Rs 30 min after NMDA treatment using the internalization assay described above. WT, GRIP2 KO, and GRIP1 and 2 DKO cortical neurons were treated with NMDA, and AMPA-Rs were allowed to undergo endocytosis/recycling for 30 min. Significantly more GluA2 and GluA3 were

retained intracellularly in GRIP1 and 2 DKO neurons compared with WT or GRIP2 KO neurons (GRIP1 and 2 DKO: GluA2: $129.5\% \pm 3.3\%$, GluA3: $169.3\% \pm 8.3\%$; GRIP2 KO: GluA2: $95.1\% \pm 6.0\%$, GluA3: $95.1 \pm 11.3\%$, relative to that of the WT, $P < 0.05$ comparing GRIP1 and 2 DKO with either WT or GRIP2 KO) ($n = 5$) (Fig. 1 C and D). This strongly suggests that GRIP1 and 2 facilitates AMPA-R recycling following NMDA-induced internalization.

To characterize the dynamics of NMDA-induced AMPA-R trafficking after GRIP1 and GRIP2 deletion, we live imaged GluA2 trafficking after NMDA treatment in individual neurons using a pH-sensitive GFP variant, ecliptic pHluorin (33). The fluorescence of pHluorin is highly pH dependent: fluorescence decreases as the pH lowers from neutrality, and eventually vanishes when pH is less than 6.0. Endocytosed AMPA-Rs are also localized at acidic compartments with a pH of ~ 5.5 for endosomes (33). Green fluorescence thus reflects the surface pH-GluA2 and can be tracked to analyze the dynamics of its trafficking (34, 35). pH-GluA2 cDNA was transfected into WT, GRIP2 KO, and GRIP1 and 2 DKO hippocampal neurons and visualized using live imaging techniques (35). Perfusion of NMDA for 5 min induced a robust yet comparable loss of pH-GluA2 fluorescence in both WT and KO neurons, which did not differ statistically between groups (WT: 0.63 ± 0.054 , GRIP2 KO: 0.68 ± 0.05 , GRIP1 and 2 DKO: 0.60 ± 0.063 , normalized to pH-GluA2 fluorescence signal before NMDA treatment) ($n = 7$) (Fig. 2 A and C). Following NMDA washout, pHluorin fluorescence recovered as these internalized receptors returned to the cell surface from endocytotic/recycling compartments (35). The kinetics of pH-GluA2 fluorescence recovery could be fit with a single exponential curve, represented by a half recovery time $T_{1/2}$. Compared with recycling in

the WT or GRIP2 KO neurons, recycling of internalized pH-GluA2 in GRIP1 and 2 DKO neurons was significantly delayed (WT $T_{1/2}$: 11.6 ± 0.8 min; GRIP2 KO $T_{1/2}$: 9.7 ± 0.33 min; GRIP1 and 2 DKO $T_{1/2}$: 20.0 ± 2.8 min, $P < 0.01$ comparing GRIP1 and 2 DKO with either WT or GRIP2 KO) ($n = 7$) (Fig. 2 B and C), consistent with the biochemical results described above. These data strongly suggest that GRIP1 and 2 regulate activity-dependent AMPA-R recycling.

Because GRIP1 affects NMDA-induced AMPA-R recycling, we examined whether GRIP1 is indeed found in endosomal compartments. For this purpose, protein markers of early and recycling endosomes were double labeled with GRIP1 by immunocytochemistry in hippocampal neurons. GRIP1 colocalized extensively with Rab11 and transferrin receptors, but not with EEA-1 (early endosome antigen-1) (Fig. 3). Rab11 is a small GTPase found exclusively in recycling endosomes (36). Transferrin receptors are also found in recycling endosomes, whereas EEA-1 is present only in early endosomes (36). Together, these data suggest that GRIP1 is localized in recycling endosomes and regulates AMPA-R recycling triggered by NMDA-R activation.

GRIP1–Sec8 Protein Complex and AMPA-R Trafficking. To facilitate the recycling of AMPA-Rs, GRIP1 likely binds additional cellular machinery to help transport AMPA-Rs to the surface. The exocyst, a multiprotein complex composed of Sec6, Sec8, Sec15, Sec3, Sec5, Sec10, Exo70, and Exo84 proteins (37), regulates exocytosis and cellular polarization by directing vesicle fusion to exocytosis sites along the plasma membrane (38). Sec8 is reported to control AMPA-R movement toward synapses via PDZ-dependent interactions (39). In addition, Sec15 is a Rab11 effector in recycling endosomes (40). Thus, the exocyst is a good candidate to partner with GRIP1 to mediate AMPA-R recycling. To test this possibility, we examined whether exocyst proteins, GRIP1, and AMPA-Rs were present in the same complex. Coimmunoprecipitation experiments from rat forebrain membranes showed that GRIP1 bound two core exocyst proteins, Sec8 and Sec6 *in vivo*, whereas GluA2 coprecipitated with GRIP1 and Sec8 (Fig. 4A). No proteins were precipitated by control IgG or by antibodies preabsorbed with their respective antigenic peptides. Moreover, GRIP1 did not bind EEA-1, consistent with our immunocytochemical data that GRIP1 is not found in early endosomes.

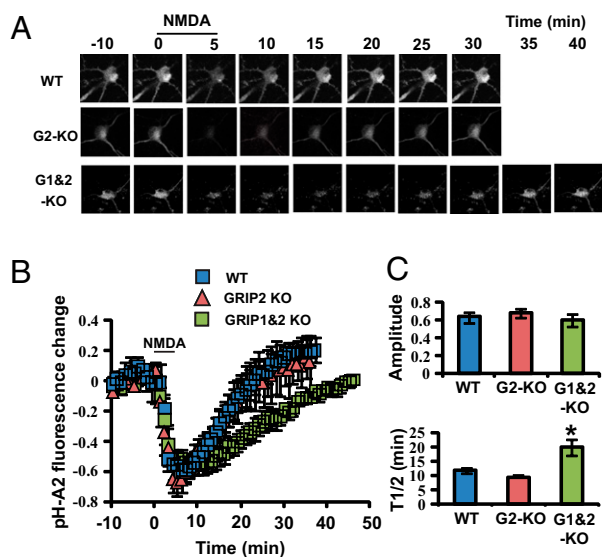


Fig. 2. NMDA-induced endocytosis and recycling of pH-GluA2 in transfected GRIP KO neurons. (A) WT, GRIP2 KO, and GRIP1 and 2 KO neurons were transfected with pH-GluA2 for image analysis, as described in the *Experimental Procedures*. Representative images of pH-GluA2 from WT, GRIP2 KO, and GRIP1 and 2 KO hippocampal neurons exposed at $t = 0$ to $20 \mu\text{M}$ NMDA for 5 min and then allowed to recover following NMDA washout. (B) Average time course of pH-GluA2 fluorescence from WT, GRIP2 KO, and GRIP1 and 2 KO hippocampal neurons during NMDA perfusion/washout experiments ($n = 7$). (C) Amplitude of pHluorin fluorescence loss at the end of NMDA perfusion, normalized to fluorescence before NMDA treatment (Upper). Recovery $T_{1/2}$ following NMDA washout (Lower). ** $P < 0.05$ compared with WT and GRIP2 KO, $n = 7$.

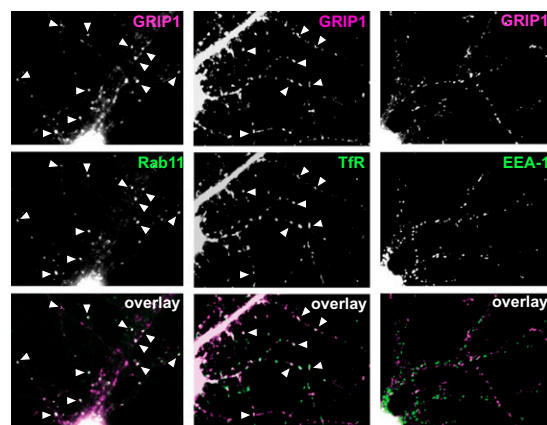


Fig. 3. GRIP1 is localized to recycling endosomes. Low-density rat hippocampal cultures (DIV21) were double labeled with anti-GRIP1 antibody (magenta) and antibodies against endosomal markers (green), including anti-Rab11 (Left), anti-transferrin receptor (Middle), or anti-EEA-1 antibody (Right). Immunofluorescence colocalizations are marked (white arrowhead) and illustrated in overlaid images (Bottom) as white signals. TfR, transferrin receptor.

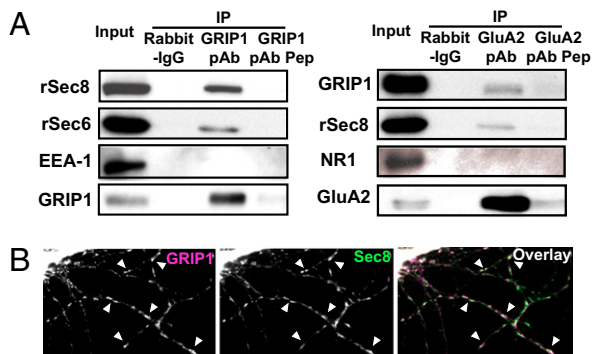


Fig. 4. GRIP1-AMPA-Rs associate with exocyst proteins in vivo. (A) Coimmunoprecipitation of GRIP1, GluA2, and exocyst proteins from rat brain. P2 membrane fraction was prepared from rat forebrain, and immunoprecipitation was performed with anti-GRIP1 or anti-GluA2 antibody. Rabbit IgG and GRIP1 or GluA2 antibody preabsorbed with their respective antigenic peptides were used as negative controls. Immunoprecipitated proteins were detected by Western blotting by probing Sec8, Sec6, and early endosome antigen-1 (EEA-1) for GRIP1 immunoprecipitation and GRIP1, Sec8, NMDA-R NR1 subunit for GluA2 immunoprecipitation. rSec8: rat Sec8, rSec6: rat Sec6. (B) Colocalization of GRIP1 and Sec8 in hippocampal neurons. Low-density cultured rat hippocampal neurons (DIV21) were fixed, permeabilized, and double-labeled with anti-GRIP1 (magenta) and anti-Sec8 (green) antibodies. Colocalization of immunofluorescence is marked (white arrowhead) and illustrated in overlay as white signals.

To further characterize the relationship between GRIP1 and the exocyst complex, we examined GRIP1 and Sec8 subcellular localization by immunocytochemistry. GRIP1 and Sec8 colocalized extensively in bead-like structures along dendrites (Fig. 4B), further supporting the model that GRIP1 and exocyst proteins are localized in the same compartments in neurons and regulate AMPA-R recycling.

Coimmunoprecipitation experiments with truncation constructs of GRIP1 revealed that transfected full-length GRIP1 and GRIP1 PDZ1-3 bound to endogenous Sec8 in HEK293T cells (Fig. S24). Sec8 did not coimmunoprecipitate with GRIP1 PDZ4-6, PDZ7, or GFP (Fig. S24). Although Sec8 possesses a C-terminal Type I PDZ-binding motif (-TTV), which mediates binding to SAP102 (41), mutation of this motif (-TTV → -TTE) did not affect Sec8 binding to GRIP1 PDZ1-3 (Fig. S24), suggesting that GRIP1–Sec8 binding is not due to a conventional PDZ domain C-terminal ligand interaction. We also mapped the interacting region of Sec8 with GRIP1 PDZ domain 1–3, and found that only full-length Sec8, and a Sec8 N-terminal construct containing the first 114 amino acids (sec8N), bound to GRIP1 PDZ1-3 (Fig. S2B).

GRIP1 modulates AMPA-R recycling following NMDA-R activation and GRIP1 directly binds Sec8, suggesting that Sec8–GRIP1 interactions might regulate AMPA-R recycling. To test this hypothesis directly, we used the GRIP1-binding region of Sec8 (Sec8N) as a dominant negative construct to disrupt endogenous GRIP1–sec8 binding in neurons. Using the same pH-GluA2 experimental paradigm, we examined the effect of Sec8N on NMDA-induced GluA2 endocytosis and recycling. Perfusion of NMDA induced rapid and comparable GluA2 internalization, as shown by pHluorin fluorescence loss (pH-GluA2: 0.69 ± 0.022 , pH-GluA2 and Sec8N: 0.60 ± 0.04 , pH-GluA2 and Sec8: 0.62 ± 0.063 , normalized to signal before NMDA treatment) ($n = 8$) (Fig. 5), suggesting that Sec8N–GRIP1 binding does not affect NMDA-induced AMPA-R endocytosis. However, similar to GRIP1 and 2 DKO neurons, cells coexpressing Sec8N protein had a greatly prolonged recycling phase. In our experiments, less than half of the internalized pH-GluA2 was recycled, making it impossible to calculate the $T_{1/2}$ value. We therefore quantitated

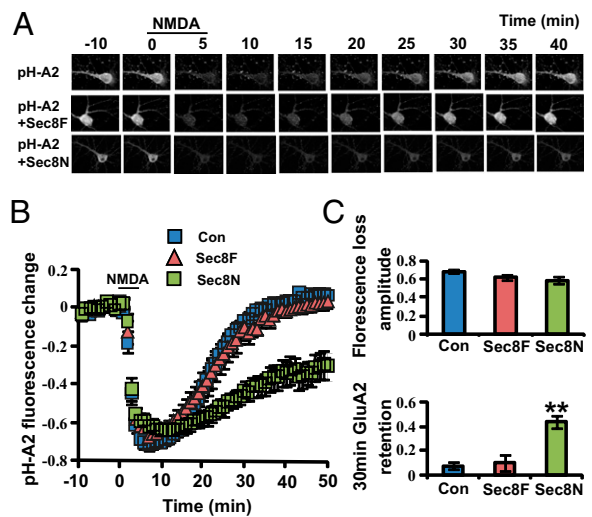


Fig. 5. NMDA-induced endocytosis and recycling of pH-GluA2 in neurons coexpressing Sec8 proteins. (A) Hippocampal neurons were transfected with pH-GluA2, pH-GluA2 and Sec8N or pH-GluA2 and Sec8 full length (Sec8F) for image analysis. Representative images of pH-GluA2 from pH-GluA2 only, pH-GluA2 and Sec8N, and pH-GluA2 and Sec8 expressing hippocampal neurons are shown during NMDA perfusion/washout experiments. (B) Average fluorescence time course of pH-GluA2 from pH-GluA2 only, pH-GluA2 and Sec8N, and pH-GluA2 and Sec8 expressing hippocampal neurons during NMDA perfusion/washout experiments. (C) Amplitude of pHluorin fluorescence loss at the end of NMDA perfusion (Upper) and the amounts of retained pH-GluA2 30 min following NMDA washout in pH-GluA2 only [Con, control (expression of pHGluA2 alone)], pH-GluA2 and Sec8N, and pH-GluA2 and Sec8 expressing neurons. (Lower). $***P < 0.001$, pH-GluA2 and Sec8N compared with pH-GluA2 only or pH-GluA2 and Sec8 group, *t* test, $n = 8$.

a single time point of 30 min after NMDA washout. Fluorescence of pH-GluA2 recovered almost completely in neurons expressing pH-GluA2 only and with Sec8 full length; however, in neurons coexpressing Sec8N, a large amount of internalized GluA2 was retained intracellularly (pH-GluA2 and Sec8N: $43.7\% \pm 5.1\%$, pH-GluA2 and Sec8: $10.4\% \pm 6.4\%$, pH-GluA2: $6.8\% \pm 3.3\%$, normalized to the signal before NMDA treatment, $P < 0.001$ pH-GluA2 and Sec8N compared with pH-GluA2 only or with Sec8 full length group) ($n = 8$) (Fig. 5). This strongly suggests that disrupting Sec8–GRIP1 interactions inhibits NMDA-R activated GluA2 recycling, further implicating endogenous Sec8–GRIP1 protein complexes in this process.

Discussion

AMPA-R function is regulated rapidly during synaptic plasticity by modulating receptor trafficking and synaptic targeting. One major mechanism that governs AMPA-R trafficking is the dynamic regulation of interactions between the receptors' intracellular C-termini and PDZ domain-containing proteins (3). GRIP1 and GRIP2 are homologous multi-PDZ domain-containing proteins that interact with the C-termini of AMPA-R GluA2 and GluA3 subunits. Although several *in vitro* studies suggest that GRIP1 and 2 regulate AMPA-R trafficking and synaptic plasticity, the role of GRIP1 and 2 in receptor trafficking is not clear. In this study, we used neuronal cultures with GRIP1 and GRIP2 genetically deleted, and found that AMPA-R recycling in response to NMDA-induced endocytosis is significantly slowed. Furthermore, GRIP1 and AMPA-R bind exocyst proteins *in vitro* and *in vivo*. Disrupting GRIP1–Sec8 interactions attenuates NMDA-induced AMPA-R recycling, in a manner similar to that observed with GRIP1 and 2 DKO neurons, suggesting that AMPA-R–GRIP1–exocyst complexes mediate activity-dependent AMPA-R trafficking.

Previous data suggest that GRIP1 and 2 may act as scaffold proteins to anchor AMPA-Rs at synapses (14, 17, 20). However, in GRIP1 and 2 DKO neurons, steady-state AMPA-R trafficking, including AMPA-R surface expression, synaptic targeting, and basal endocytosis, was not affected. This argues against a model in which GRIP proteins maintain AMPA-Rs at synapses. Furthermore, we found that GRIP1 colocalizes extensively with Rab11 and transferrin receptor in recycling endosomes, suggesting that GRIP1 has a more dynamic function. The disparity between our findings and previous studies may result from experimental system differences: We examined neurons with acute genetic deletions of GRIP1 and GRIP2, whereas other studies used more indirect techniques, such as overexpression, mutagenesis, or peptide perfusion.

NMDA-R activation by bath application of NMDA in cultured neurons triggers rapid endocytosis of AMPA-Rs and reduces synaptic transmission efficacy. This process involves signaling mechanisms shared with LTD in brain slices and thus is regarded as a model of LTD (27, 30). In GRIP1 and 2 DKO neurons, AMPA-R endocytosis following NMDA treatment was not affected, but the recycling process was greatly prolonged. This change of kinetics on AMPA-R trafficking would modify neuronal transmission in a time-dependent manner, thereby conferring temporal specificity to synaptic plasticity. No slowing of AMPA-R recycling was observed in GRIP2 single KO neurons. However, GRIP2 may still be involved in this process, as GRIP1 and GRIP2 may compensate for each other's functions. Indeed, in cerebellar Purkinje neurons, although GRIP1 and 2 DKO eliminates LTD, either GRIP1 or GRIP2 is sufficient to allow LTD (25).

Besides GRIP proteins, the GluA2 C terminus also binds another PDZ domain-containing protein, PICK1. Competition between GRIP1 and 2 and PICK1 for the same GluA2 binding site is regulated by PKC-mediated phosphorylation of GluA2 at Ser880, which abolishes GRIP–GluA2 interaction without affecting PICK1–GluA2 interactions (10, 12). GluA2 Ser880 phosphorylation and subsequent binding of AMPA-Rs to PICK1 are implicated in mediating cerebellar LTD by triggering AMPA-R endocytosis (7, 42). In hippocampal neurons, live imaging studies suggest that GluA2 Ser880 phosphorylation and association of receptors with PICK1 retains internalized AMPA-Rs intracellularly (35). Our study reveals that GRIP1 acts in the opposite direction, facilitating reinsertion of internalized AMPA-Rs back to the surface. Previous studies show that PKC-dependent phosphorylation of GluA2 Ser880 acts as a switch to transfer AMPA-Rs from PICK1 to GRIP proteins during cerebellar LTD (7, 42) or NMDA-induced AMPA-R trafficking (24, 35). Taken together, we propose a model that PICK1 binding to phospho-GluA2 inhibits AMPA-R recycling, whereas GRIP1 binding to dephospho-GluA2 enhances recycling of internalized AMPA-Rs back to the surface.

Internalized AMPA-Rs must be coupled to protein transport and exocytosis machinery to recycle back to the surface. GRIP1 may serve as a platform to link AMPA-Rs to such machinery, as we detected GRIP1, AMPA-Rs and exocyst proteins in the same protein complex in the brain. The exocyst protein Sec8 is implicated in transporting AMPA-Rs to synapses, whereas Exo70, another exocyst component, mediates receptor synaptic accumulation (39). Disruption of GRIP1–Sec8 binding severely inhibits AMPA-R recycling in response to NMDA-R activation. Inhibition by dominant negative Sec8 is even more prominent than that seen with GRIP1 deletion, implying that Sec8 acts downstream of GRIP1 to mediate AMPA-R recycling and that additional pathways besides GRIP1 may regulate AMPA-R recycling via the exocyst complex. Consistent with this hypothesis, exocyst proteins control exocytosis sites at cell membranes (38), as well as Rab11 function at recycling endosomes (40). This suggests that GRIP1–exocyst complexes may regulate AMPA-R trafficking in multiple subcellular locations.

Experimental Procedures. Experimental methods are described briefly here. Full details are contained in *SI Experimental Procedures*. Use and care of animals in this study abided by the guidelines of the Institutional Animal Care and Use Committee at the Johns Hopkins University.

cDNA Subcloning and lentiviral preparation. pH-GluA2, GFP-GRIP1 constructs, and Sec8 constructs were PCR amplified and subcloned into expression vectors. Cre-lentiviruses were generated as described elsewhere (25).

Neuronal cell culture, plasmid transfection, and imaging. Neuronal cultures were prepared and maintained as previously described (35). Plasmids were transfected into neurons with lipofectamine. Live images of pH-GluA2 were obtained using a Zeiss LSM 510 Meta/NLO system (35).

Biochemical analysis from rat brains and cells. Rat brain subcellular fractionation and coimmunoprecipitation experiments are described in *SI Experimental Procedures*. Biotinylation assays of AMPA-R trafficking were performed as described elsewhere (27).

Statistical Analysis. All immunoprecipitation experiments were conducted three times. Every neuronal biotinylation assay was conducted at least twice, each containing three separate plates from the same culture batch. pH-GluA2 live images were acquired from multiple coverslips from two to four culture batches. Data are expressed as mean \pm SEM unless otherwise specified. Statistical significance was determined by unpaired two-tailed Student *t* test. Statistical level is stated in figure legends.

ACKNOWLEDGMENTS. We thank Monica Coulter for excellent technical assistance and Sandy Yu for preparing mice for culture. This work was supported by National Institutes of Health Grant R01NS036715. R.L.H. is an investigator with the Howard Hughes Medical Institute.

- Malinow R, Malenka RC (2002) AMPA receptor trafficking and synaptic plasticity. *Annu Rev Neurosci* 25:103–126.
- Kerchner GA, Nicoll RA (2008) Silent synapses and the emergence of a postsynaptic mechanism for LTP. *Nat Rev Neurosci* 9:813–825.
- Shepherd JD, Huganir RL (2007) The cell biology of synaptic plasticity: AMPA receptor trafficking. *Annu Rev Cell Dev Biol* 23:613–643.
- Dong H, et al. (1997) GRIP: A synaptic PDZ domain-containing protein that interacts with AMPA receptors. *Nature* 386:279–284.
- Srivastava S, et al. (1998) Novel anchorage of GluR2/3 to the postsynaptic density by the AMPA receptor-binding protein ABP. *Neuron* 21:581–591.
- Xia J, Zhang X, Staudinger J, Huganir RL (1999) Clustering of AMPA receptors by the synaptic PDZ domain-containing protein PICK1. *Neuron* 22:179–187.
- Chung HJ, Steinberg JP, Huganir RL, Linden DJ (2003) Requirement of AMPA receptor GluR2 phosphorylation for cerebellar long-term depression. *Science* 300:1751–1755.
- Dong H, et al. (1999) Characterization of the glutamate receptor-interacting proteins GRIP1 and GRIP2. *J Neurosci* 19:6930–6941.
- Osten P, et al. (1998) The AMPA receptor GluR2 C terminus can mediate a reversible, ATP-dependent interaction with NSF and alpha- and beta-SNAPs. *Neuron* 21:99–110.
- Chung HJ, Xia J, Scannevin RH, Zhang X, Huganir RL (2000) Phosphorylation of the AMPA receptor subunit GluR2 differentially regulates its interaction with PDZ domain-containing proteins. *J Neurosci* 20:7258–7267.
- Matsuda S, Mikawa S, Hirai H (1999) Phosphorylation of serine-880 in GluR2 by protein kinase C prevents its C terminus from binding with glutamate receptor-interacting protein. *J Neurochem* 73:1765–1768.
- Xia J, Chung HJ, Wihler C, Huganir RL, Linden DJ (2000) Cerebellar long-term depression requires PKC-regulated interactions between GluR2/3 and PDZ domain-containing proteins. *Neuron* 28:499–510.
- Brückner K, et al. (1999) EphrinB ligands recruit GRIP family PDZ adaptor proteins into raft membrane microdomains. *Neuron* 22:511–524.
- Wyszynski M, et al. (2002) Interaction between GRIP and liprin-alpha/SYD2 is required for AMPA receptor targeting. *Neuron* 34:39–52.
- Stegmüller J, Werner H, Nave KA, Trotter J (2003) The proteoglycan NG2 is complexed with alpha-amino-3-hydroxy-5-methyl-4-isoxazolepropionic acid (AMPA) receptors by the PDZ glutamate receptor interaction protein (GRIP) in glial progenitor cells. Implications for glial-neuronal signaling. *J Biol Chem* 278:3590–3598.
- Takamiya K, et al. (2004) A direct functional link between the multi-PDZ domain protein GRIP1 and the Fraser syndrome protein Fras1. *Nat Genet* 36:172–177.

